Large-area self assembled monolayers of silica microspheres formed by dip coating

Y. Wang[1,2*], L. Chen[1], H. Yang[1], Q. Guo[3], W. Zhou[1], M. Tao[1,3]

[1]Department of Electrical Engineering, NanoFAB Center, University of Texas at Arlington, Arlington, TX 76019-0072, USA

[2]Department of Chemistry and Biology, University of Electronic Science and Technology of China, Zhongshan Institute, Zhongshan 528402, China

[3]ZT Solar, Inc., 1120 South Freeway, Fort Worth, TX 76104, USA

Formation by dip coating of highly ordered and closely packed, self assembled monolayers (SAMs) of microsized silica spheres has been reported. Under optimized coating conditions, SAMs were formed with 2 μm diameter silica spheres on record-breakingly large areas, measuring 3×10 mm^2 on silicon substrates and 1.5×11 mm^2 on glass substrates. The SAMs structure and their spatial extension were significantly influenced by the concentration of the solution, withdrawal speed, immersion time, relative humidity, types of solvent and substrate material. The SAMs of silica microspheres provide a glimpse into the wide range of photonic applications for dip coating such as surface texturing and anti-reflection coatings.

Keywords: *self assembled monolayer; silica microsphere; dip coating*

1. Introduction

Solution prepared omnidirectional antireflection (omni-AR) coatings were recently investigated both experimentally and theoretically, in order to improve the coupling of sunlight into solar cells [1, 2]. The basic structure of the omni-AR coating comprises an array of hemispherical microparticles of an optically transparent dielectric material. The hemispherical particles are formed by partially immersing spherical particles in a dielectric layer with a thickness lower than the diameter of the microspheres. The unique way the omni-AR coating is formed allows it to be prepared from solutions, which is inherently low cost. The hemispherical shape of the omni-AR coating makes sunlight collection less dependent on the incident angle of sunlight, from sunrise to sunset. The formation of the omni-AR coating on solar cells requires a simple assembly process for large area closely packed monolayers of microspheres.

_____

*Corresponding author, e-mail: wangzsedu@126.com

Report Documentation Page		

1. REPORT DATE **2010**	2. REPORT TYPE	3. DATES COVERED **00-00-2010 to 00-00-2010**

4. TITLE AND SUBTITLE	5a. CONTRACT NUMBER
Large-area self assembled monolayers of silica microspheres formed by dip coating	5b. GRANT NUMBER
	5c. PROGRAM ELEMENT NUMBER
6. AUTHOR(S)	5d. PROJECT NUMBER
	5e. TASK NUMBER
	5f. WORK UNIT NUMBER

7. PERFORMING ORGANIZATION NAME(S) AND ADDRESS(ES) **Department of Electrical Engineeering,NanoFAB Center,University of Texas at Arlington,Arlington,TX,76019**	8. PERFORMING ORGANIZATION REPORT NUMBER

9. SPONSORING/MONITORING AGENCY NAME(S) AND ADDRESS(ES)	10. SPONSOR/MONITOR'S ACRONYM(S)
	11. SPONSOR/MONITOR'S REPORT NUMBER(S)

12. DISTRIBUTION/AVAILABILITY STATEMENT
Approved for public release; distribution unlimited

13. SUPPLEMENTARY NOTES

14. ABSTRACT
Formation by dip coating of highly ordered and closely packed, self assembled monolayers (SAMs) of microsized silica spheres has been reported. Under optimized coating conditions, SAMs were formed with 2 μm diameter silica spheres on record-breakingly large areas, measuring 3?0 mm2 on silicon substrates and 1.5?1 mm2 on glass substrates. The SAMs structure and their spatial extension were significantly influenced by the concentration of the solution, withdrawal speed, immersion time, relative humidity, types of solvent and substrate material. The SAMs of silica microspheres provide a glimpse into the wide range of photonic applications for dip coating such as surface texturing and anti-reflection coatings.

15. SUBJECT TERMS
self assembled monolayer; silica microsphere; dip coating

16. SECURITY CLASSIFICATION OF:			17. LIMITATION OF ABSTRACT	18. NUMBER OF PAGES	19a. NAME OF RESPONSIBLE PERSON
a. REPORT **unclassified**	b. ABSTRACT **unclassified**	c. THIS PAGE **unclassified**	**Public Release**	**12**	

Self-assembly is a spontaneous formation of ordered structures caused by interactions between the particles. Well ordered, self assembled monolayers (SAMs) of nanoparticles/microparticles attract increasing interest because of their significance for photonic crystals [3, 4], optoelectronic devices [5, 6], sensors [7, 8], coatings [9–12] and other applications [13–16]. Many practical devices require monolayers with ordered structures over large areas. Several self assembly processes have been proposed, including physical, chemical, layer-by-layer, molecular and evaporation induced self assemblies [17–23]. However, most self assembly research focuses on nanoparticles and modifications of their surface properties (e.g., organic ligands or surface charge). The introduction of organic compounds in the omni-AR coating for solar cell applications can lead to increased absorption and instability under constant ultraviolet radiation.

Dip coating is a popular self assembly process, in which a substrate is slowly withdrawn from a colloidal suspension and a uniform liquid film containing particles is formed on it. As the film thickness becomes lower than twice the particle diameter, due to solvent evaporation, the vertical component of the capillary forces drags the particles downwards to the substrate where they self assemble into ordered structures [19]. The mass transfer process simultaneously occurs over the entire substrate, ensuring a high process throughput. Recent experiments revealed the microscopic mechanism governing the formation of layered arrays of latex microparticles on glass substrates and silica/latex nanoparticles on glass/silicon substrates [9, 19–23]. However, the parameters that govern the self assembly process were not completely quantified, and no procedure has yet been proposed for obtaining monolayer arrays of microspheres over large areas and with few defects (e.g., voids and multilayers). On the other hand, bilayers start to form above a critical coverage of monolayer, whereas voids remain [24].

As summarized above, little has been published on the feasibility of dip coating for the formation of large area monolayers of microsized silica spheres, without the addition of organic compounds for surface modification. In the paper, the authors report on record breaking large areas of highly ordered and closely packed monolayers of silica microspheres, having dimensions of 3×10 mm^2 and 1.5×11 mm^2 on silicon (Si) and glass substrates, respectively. The spatial extension of these self assembled structures can be further increased, but depends on the volume of the solution. This process takes place at room temperature under ambient conditions without substrate pretreatment. The influence of the microsphere concentration, withdrawal speed, relative humidity and substrate immersion time, properties of solvent and substrate material on SAMs of silica microspheres is also revealed.

2. Experimental

Materials. Monodispersed plain silica mircospheres having the diameter of 2 μm were supplied by Microspheres-Nanospheres, the Corpuscular Company. The suspension was used without further purification. 1 mm thick glass slides from Fisher Scien-

tific and 500 µm thick silicon wafers from Nova Electronic Materials were used as substrates in the experiments. These substrates were cleaned by immersing them into a solution containing 30% H_2O_2 and 70% H_2SO_4 under ambient conditions for 24 h, then rinsing them with deionized water, and drying with dry N_2, before commencing the dipping coating process.

Formation of monolayers. SAMs of silica mircospheres were obtained by dipping silicon/glass substrates into a well dispersed silica mircosphere suspension. Before dipping, the suspension was dispersed in an ultrasonic bath and with a magnetic stirrer. During the coating process, the substrate was vertically dipped into the suspension for a few minutes and withdrawn at a programmed speed. The wet coating adhering to the substrate was subsequently air dried under ambient conditions. The coating parameters were: concentration of the suspension (5–27 wt. %), withdrawal speed (0.11 –5.35 mm/s), immersion time (1–6 min), relative ambient humidity (20–80%) and type of solvent (ethanol, water and ethanol/water 1:1 mixture). The temperature was fixed at 20 °C for all the experiments.

The formed SAMs of silica mircospheres were characterized with a Zeiss SUPRA 55VP scanning electron microscope (SEM), a Nikon LV100 optical microscope with a digital camera and optical diffraction pattern measurements. The surface coverage of the silica microsphere monolayers was calculated by directly counting the particle area using image analysis software. The criterion used to calculate the monolayer surface coverage was the ratio between the two dimensionally projected area of the silica microspheres and the substrate area.

3. Results and discussion

A series of SEM images taken at the same location but under various magnifications, as well as an optical microscope image, are shown in Fig. 1. The coating has a closely packed hexagonal structure and is sufficiently uniform, with a few voids in the monolayer (Figs. 1b–d). This can be illustrated by a two-dimensional fast Fourier transformation (FFT) and the well defined laser diffraction patterns in transmitted mode (Fig. 1f) [8]. Sharp peaks in the FFT confirm the presence of long range SAM order, and a set of regular, periodic hexagonal configuration of symmetrical spots, illuminated with a pinhole of diameter 0.50 mm in Fig. 2f confirms the microscopy observations that the sizes of the larger domains in the monolayer samples were about 500 µm.

It should be noted that the hexagonal closely packed structure is not formed everywhere over the substrate, in this case. A small area of multilayers and accumulation of microspheres and submonolayers with non-connected stripes and loosely packed islands can be observed at the bottom of the substrate (Fig. 2a) and sub-monolayers with short range ordering and loosely packed islands are visible at the top of the substrate (Fig. 2b). This is attributed to interactions of all the factors: evaporation, capillary forces, particle–particle interactions, particle–substrate interactions, concentration gradient in the suspension, etc.
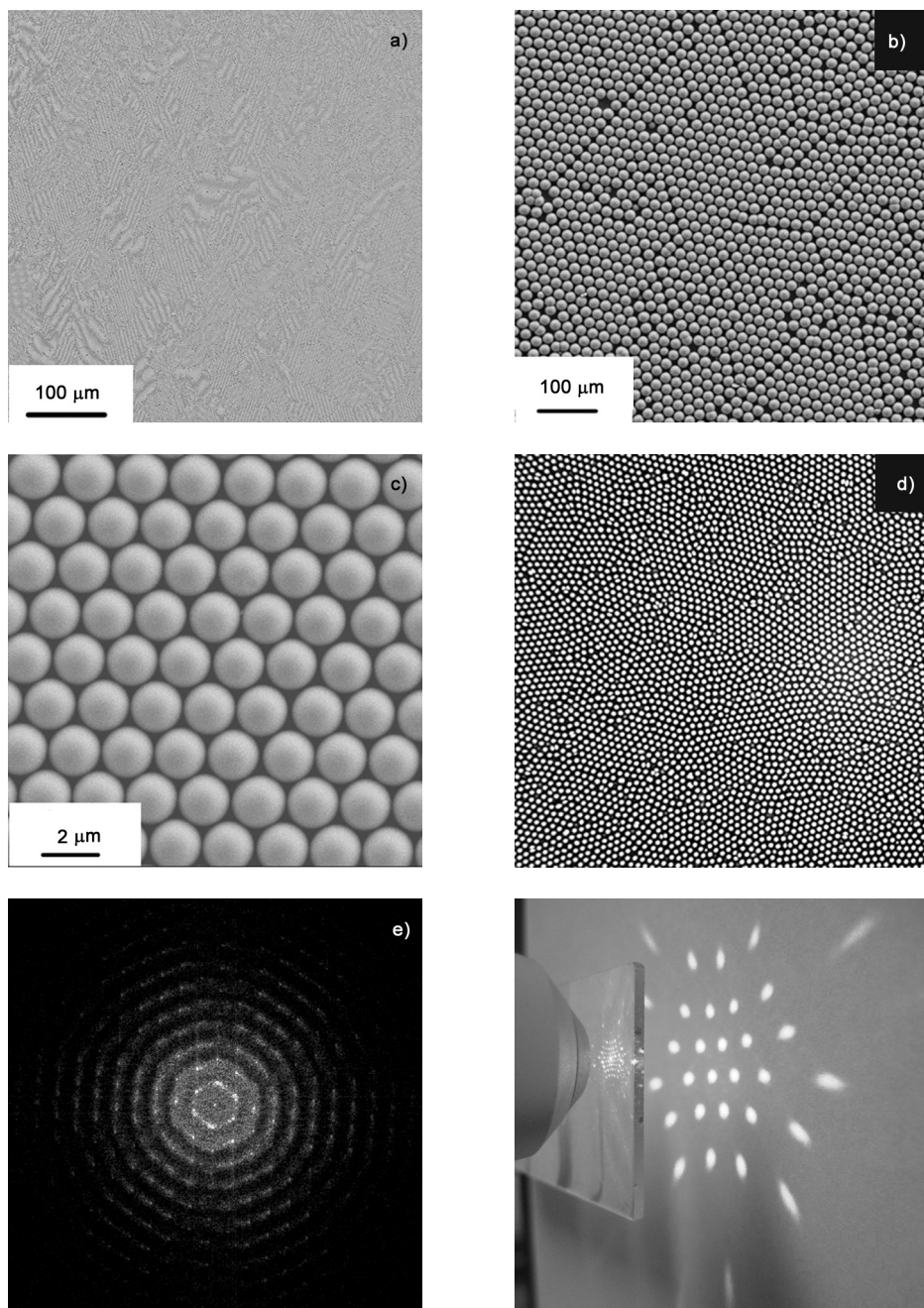
Fig. 1. Series of SEM images (a)–(c) with various magnifications, d) large area SAM
on a silicon substrate under optical microscope showing a, e) two-dimensional Fourier transform
pattern of a low-magnification SEM image, f) diffraction pattern of a green laser beam transmitted
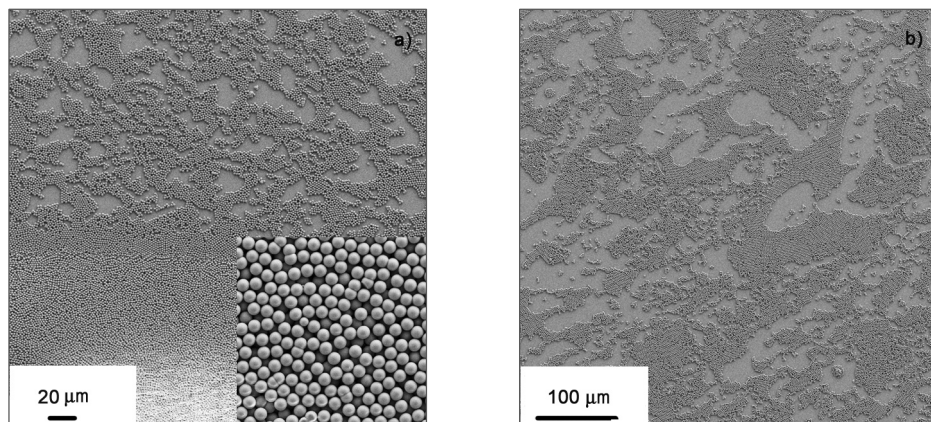through a uniform hexagonally packed monolayer on a glass substrate

Fig. 2. SEM images at the bottom (a) and top (b) of the substrate and high-magnification
SEM image of the same location (insert in (a))

Figure 3 illustrates the process of dip coating, driven by the convective flux generated by the evaporation of solvent in the meniscus region and the lateral capillary forces. The particle size and density influence the balance among various elements. Successive particle arrays are expected to form continuously as the particle flux fills up the meniscus [20, 21]. The attraction by the lateral capillary force leads to a dense hexagonal packing. At the same time, the upward flux of particles undergoes particle–particle interactions and particle–substrate interactions.
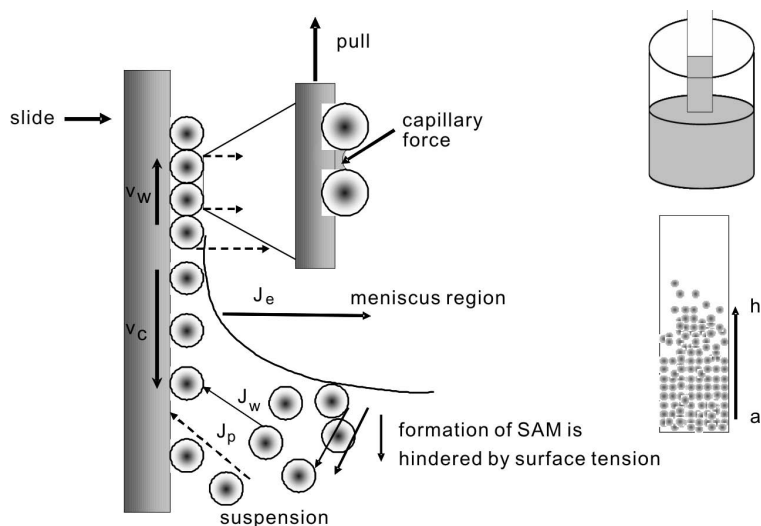

Fig. 3. Scheme of the dip coating mechanism, where various forces interact
with each other to form self assembled coated structures: V_w – substrate
withdrawal rate, V_c – monolayer growth rate, J_e – evaporation flux of solvent,
J_w, J_p – entering fluxes of particles and solvent, respectively

In our experiments, the concentration gradient of silica microspheres in the suspension by gravity resulted in different upward fluxes of particles at different heights of the suspension, insufficient convective flux at the top of the suspension and superfluous convective flux at the bottom of the suspension, thus forming different structural characterizations on the substrate. Note that the coating area is limited by the volume of the solution. In our experiments, only 20 cm^3 of suspension is used, which corresponds to a maximum immersion depth of 16 mm for the substrate. Under optimum coating conditions, SAMs were formed with 2 μm diameter silica spheres at record-breaking large areas of $3{\times}10$ mm^2 on silicon substrates and $1.5{\times}11$ mm^2 on glass substrates.
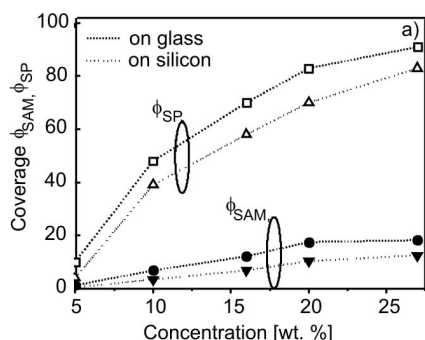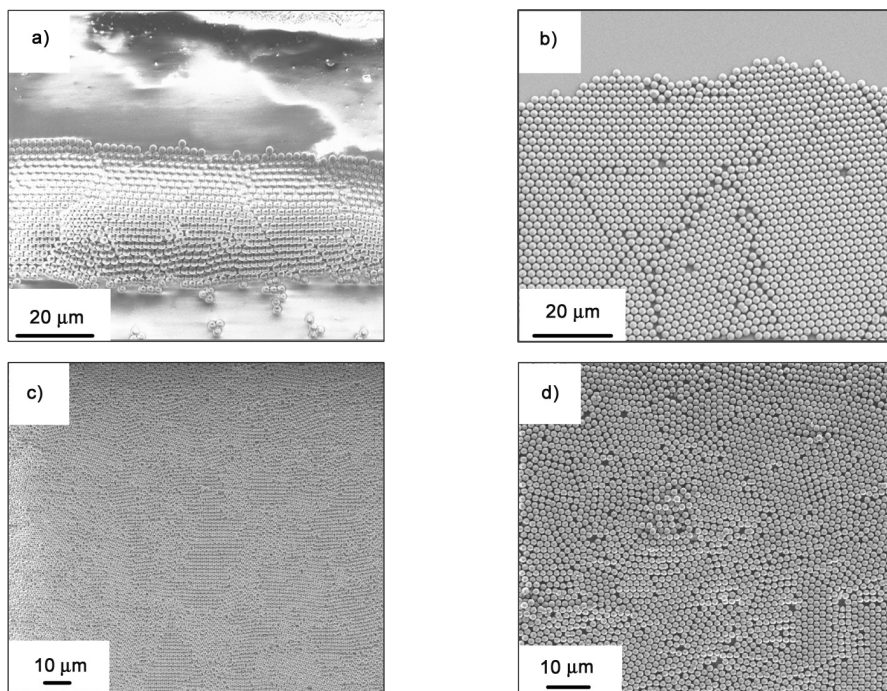

Fig. 4. SEM images of SAMs structures on glass substrates with ethanol dispersed silica microspheres of the concentrations [wt. %]: a) 5, b) 10, c) 20, d) 27, e) microsphere surface coverage Φ_{SP} and SAMs surface coverage Φ_{SAM} on glass and silicon substrates

The impact of the particle concentration in the coating solution was investigated first by varying it from 5 to 27 wt. %, with all other parameters kept constant. Fig-

ure 4e shows the results of the surface coverage of silica microspheres adhered onto the substrate surface, Φ_{SP}, and the surface coverage of the well ordered, closely packed SAMs of silica microspheres on the substrate surface, Φ_{SAM}, for various particle concentrations. With the increase in the particle concentration from 5 wt. % to 20 wt. %, both Φ_{SP} and Φ_{SAM} obviously increased. A further increase in the microsphere concentration, to 27 wt. %, clearly increased Φ_{SP}, but Φ_{SAM} increased only slightly. The structural characterization of self assembled silica microspheres was observed by SEM (Fig. 4a–d). Well ordered closely packed SAMs film is obtained with the 20 % concentration of silica microspheres (Fig. 4c). When the particle concentration is high, more particles adhere to the substrate and large area SAMs are easy to form (Fig. 4d). However, when the particle concentration is low, insufficiently many particles are supplied for a monolayer to form, resulting in scattered stripes (Fig. 4a, b). The conclusion from these experiments is that in dip coating, a proper concentration needs to be found for the fabrication of highly uniform closely packed SAMs of silica microspheres. This is because the concentration of particles in the suspension determines the upward flux of particles, for a given convective flux of liquid [20, 23].
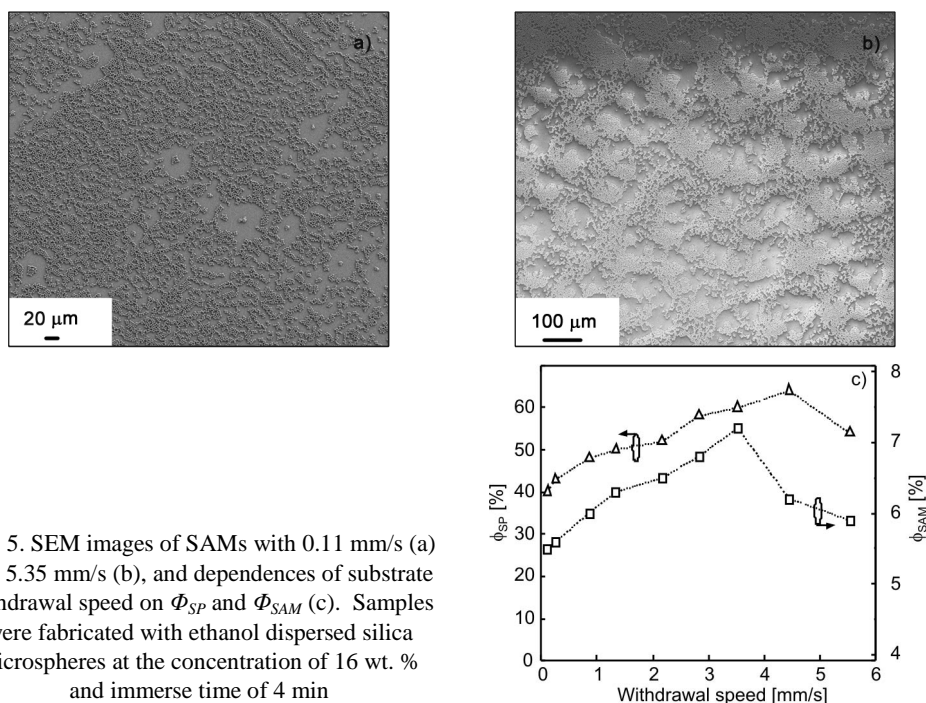

Fig. 5. SEM images of SAMs with 0.11 mm/s (a) and 5.35 mm/s (b), and dependences of substrate withdrawal speed on Φ_{SP} and Φ_{SAM} (c). Samples were fabricated with ethanol dispersed silica microspheres at the concentration of 16 wt. % and immerse time of 4 min

The substrate withdrawal speed, immersion time, relative humidity, type of solvent and substrate material were also investigated. Figure 5c shows the dependence of Φ_{SP} and Φ_{SAM} on the withdrawal speed. The samples were fabricated with ethanol dispersed silica microspheres at the concentration of 16 wt. % and 4 min immersion time. When the withdrawal speed increased from 0.11 to 3.53 mm/s, both Φ_{SP} and Φ_{SAM}

increased. A low withdrawal speed of 0.11 mm/s resulted in stripes of tens or hundreds of microspheres randomly scattered on the substrate (Fig. 5a). The microspheres in the stripes exhibited chaining and short range ordering. This structure was probably formed when the microspheres in the drying film were attracted to each other by capillary forces. Furthermore, narrow regions of multilayers were formed at the bottom of the substrate. Increasing the withdrawal speed resulted in better SAMs of silica microspheres with improved ordering and fewer voids. The stripes began to coalesce into a uniform ordered domain. With withdrawal speed exceeding 3.53 mm/s, Φ_{SAM} began to decrease but Φ_{SP} continued to increase up to a withdrawal speed of 4.45 mm/s. At the withdrawal speed of 5.35 mm/s, only a narrow region of well ordered SAMs was formed at the bottom of the substrate. Beyond that, long stripes and voids were observed, and were probably caused by the extremely rapid withdrawal speed (Fig. 5b). At a more suitable withdrawal speed, the upper region of the meniscus retreats below the height of the particles as the solvent evaporates, exposing the particles. At this moment, the microspheres experience an attractive lateral capillary force from the substrate, allowing the particles to be self assembled into an ordered monolayer array.

The consequences of selecting the optimum immersion time and the optimum relative humidity on the Φ_{SP} and Φ_{SAM} of silica microspheres are shown in Fig. 6. Both Φ_{SP} and Φ_{SAM} increased at first, and then decreased as both the optimum immersion time and the relative humidity were increased. The optimum immersion time of 4 min and relative humidity of 40% were found to yield a maximum for the Φ_{SP}. We observed in our experiments that gravity caused the silica microspheres to sink to the bottom of the suspension, resulting in a concentration gradient of silica microspheres in the suspension. Improved stability of the silica microsphere suspension is important to obtain large area well ordered and closely packed SAM of silica microspheres. For our applications, organic surfactants for the prevention of sedimentation were purposely avoided, since the coating should be fully inorganic in order to achieve the desired transparency and reliability [2].
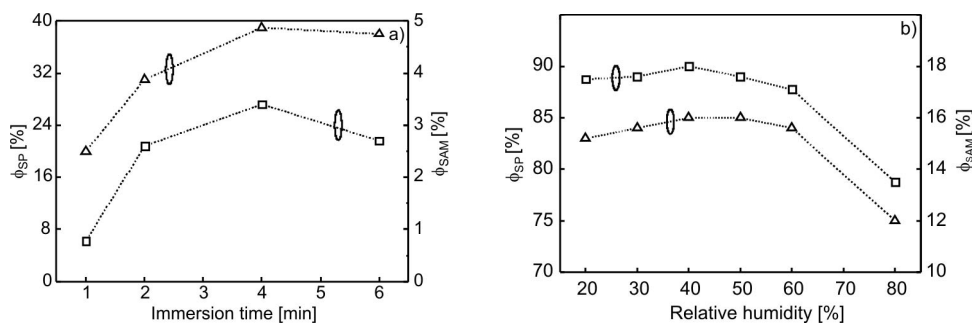

Fig. 6. The impact of the immersion time (a) and the relative humidity (b) on the coating coverage Φ_{SP} and Φ_{SAM}. Samples were fabricated with ethanol-dispersed silica microspheres with 16 wt. % (a) and 20 wt. % concentration (b), 4 min immersion time, and at ambient conditions on the glass substrate

The relative humidity controls the evaporation rate, which affects the motion of particles on the substrate. Figure 7 shows the scheme of impact of the evaporation rate

on the convective flux during dip coating. With low humidity, the evaporation rate is fast, and large convective flux accelerates particles to quickly stick to the substrate before an ordered structure can be achieved. At the same time, the particle flux into the meniscus increases, leading to faster array formation (Fig. 7a). For high humidity and low evaporation rate, the meniscus is thick and no sufficient convective flux exists to force particles upward (Fig. 7b). The particle concentration in the meniscus remains low and surface coverage by silica microspheres decreases.
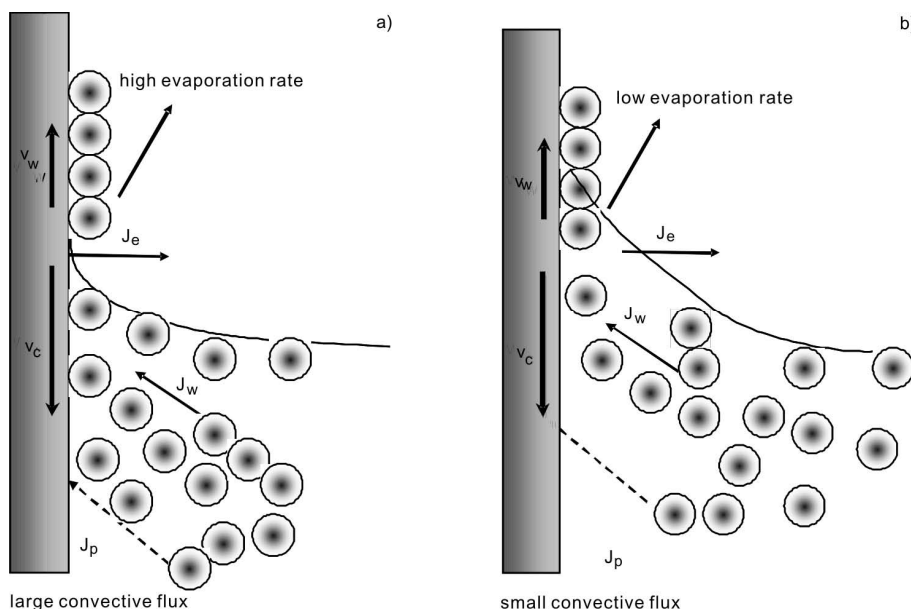

Fig. 7. Impact of the evaporation rate on the convective flux during dip coating

Figure 8 shows the impact of solvent type on SAMs structure. The samples were fabricated at the concentration of 10 wt. %, withdrawal speed 2.82 mm/s and immersion time 2 min on glass substrates. The solvent controls surface tension, evaporation rate and stability of the suspension. When the solvent was ethanol, multilayers were observed at the bottom of the substrate (bottom of Fig. 8a), in addition to well-ordered closely packed SAM structures in the centre. This may be due to fast solvent evaporation as well as high densities of microspheres towards the bottom of the substrate. On the other hand, a disordered loosely packed region was observed above the closely packed region (top of Fig. 8a). Φ_{SP} and Φ_{SAM} increased obviously in the aqueous solution (Fig. 8b), and a large area uniform closely packed SAMs region (centre in Fig. 8b) was sandwiched by loosely-packed monolayer regions, specifically between an upper monolayer and a lower one. The optimum condition for achieving large area well ordered and closely packed SAMs (Fig. 8c) was identified, namely a 1:1 mixture of ethanol and water. This is believed to an optimum balance between solvent evaporation and particle interactions. In the case of water, a solvent with high surface ten-

sion leads a thick meniscus to form, just as shown in Fig. 7a. No sufficient convective flux exists to force the particles upward, since the evaporation of solvent takes longer time. At the same time, the meniscus can still be maintained as the substrate is withdrawn. It is likely that the meniscus breaks into droplets due to its gravity, forming many stripes and islands. In the case of ethanol, a solvent with low surface tension results in a thin meniscus and quick evaporation, as shown in Fig. 7b. Although particles are supplied towards the meniscus, the capillary force between particles is insufficient for the formation of closely packed SAMs over large areas, because of the low surface tension [23].
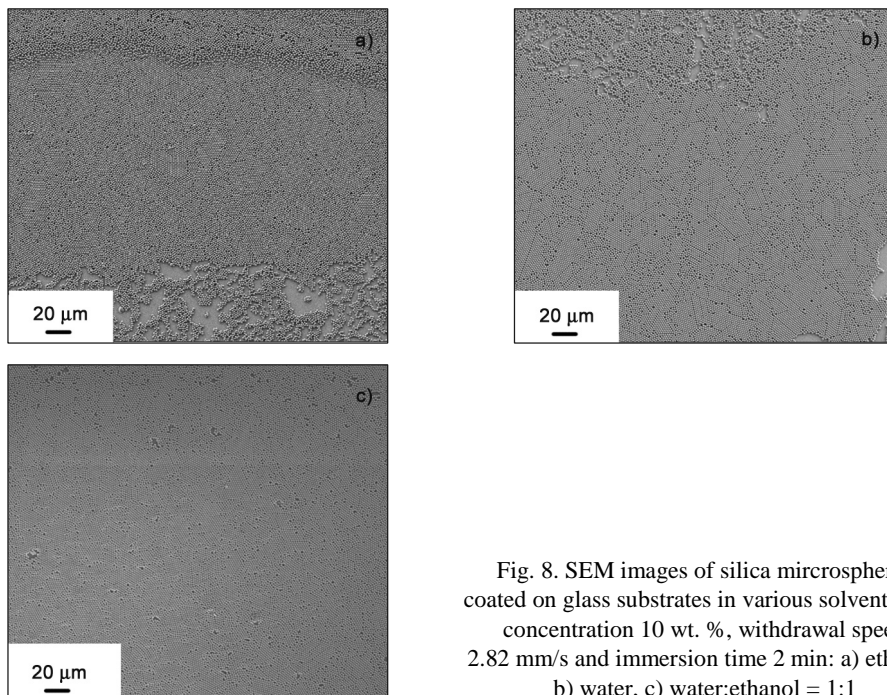

Fig. 8. SEM images of silica mircrospheres coated on glass substrates in various solvents with concentration 10 wt. %, withdrawal speed 2.82 mm/s and immersion time 2 min: a) ethanol, b) water, c) water:ethanol = 1:1
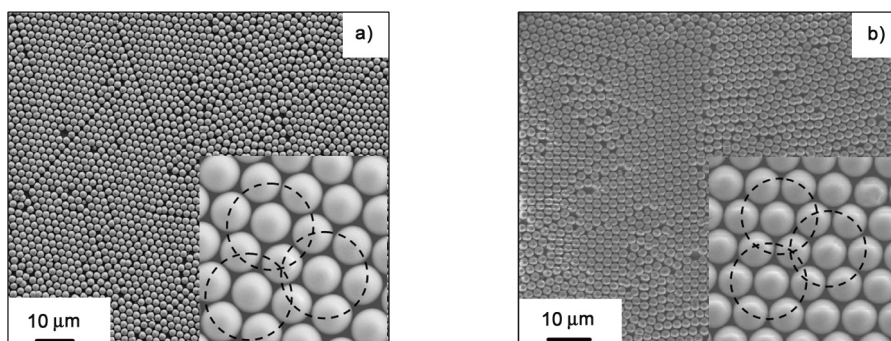

Fig. 9. SEM images of ethanol dispersed silica microspheres with concentration 20 wt. %, immersion time 4 min, relative humidity 40%, and withdrawal speed 2.82 mm/s on (a) silicon and (b) glass substrates

Seen from Fig. 4a, Φ_{SP} and Φ_{SAM} on glass substrates were higher than those on silicon substrates, indicating that the microspheres adhere better to glass than to silicon. Strong interactions between particles and glass probably resulted in more particles binding to the surface of glass, with each microsphere touching six neighbouring microspheres in the monolayer. The average separation of neighbouring microspheres was estimated, and found to be roughly 97 nm on glass substrates and 118 nm on silicon substrates (Fig. 9). This indicates that microspheres can be packed more closely together on glass substrates than on silicon substrates. However, the SAMs structures on glass and silicon substrates are very similar, as seen in Fig. 9.

4. Conclusions

We have demonstrated large area, self assembled monolayers of silica microspheres with the diameter of 2 μm by dip coating, forming uniform well ordered and closely packed SAM structures over areas of 3×0 mm^2 on silicon substrates and 1.5×11 mm^2 on glass substrates. The self assembled structure and its spatial extension are significantly influenced by the concentration of silica microspheres in the suspension, substrate withdrawal speed, substrate immersion time, relative humidity, solvent type and substrate material. A rapid formation of self assembled monolayers of silica microsphere provides a glimpse into a wide range of photonic applications of dip coating, such as large area surface texturing for antireflection coatings in solar cells.

References

[1] TAO M., ZHOU W., YANG H., CHEN L., Appl. Phy. Lett., 91 (2007), 081118.
[2] ZHOU W., TAO M., YANG H.CHEN L., J. Appl. Phys., 102 (2007), 103105.
[3] VAN BLAASEREN A., RUEL R., WILTZIUS P., Nature, 385 (1997), 321.
[4] HAN S.E., STEIN A., NORRIS D., Phys. Rev. Lett., 99 (2007), 053906.
[5] NIGHT J.C., BROGENG J., BIRKS T.A., RUSSEL P.S.J., Science, 282 (1998), 1476.
[6] CHO A., Science, 299 (2003), 1685.
[7] HOLTZ J.H., ASHER S.A., Nature, 389 (1997), 829.
[8] PREVO B.G., VELEV O.D., Langmuir, 20 (2004), 2099.
[9] PREVO B.G., HON E.W., VELEV O.D., J. Mater. Chem., 17 (2007), 791.
[10] PREVO B.G., HWANG Y., VELEV O.D., Chem. Mater., 17 (2005), 3642.
[11] ARSENAULT A.C., MIGUEZ H., KITAEV V., OZIN G.A., MANNERS I., Adv. Mater. 15 (2003), 503.
[12] LIN S.Y., FLEMING J.G., EL-KADY I., BISWAS R., HO K.M., J. Opt. Soc. Am. B, 20 (2003), 1538.
[13] CASSAGNEAU T., CARUSO F., Adv. Mater. 14 (2002), 1629.
[14] GOPIDAS K.R., BOHORQUEX M., KAMAT P.V., J. Phys. Chem. 94 (1990), 6435.
[15] WANG D., MÖHWALD H., Adv. Mater. 16 (2004), 244.

[16] HULTEEN J.C., VAN DUYNE R.P., J. Vac. Sci. Technol. A, 13 (1995), 1553.

[17] SHERRINGTON D.C., TASKINEN K.A., Chem. Soc. Rev. 30 (2001), 83.

[18] PARK S.H., XIA Y., Chem. Mater. 10 (1998), 1745.

[19] MICHELETTO R., FUKUDA H., OHTSU M., Langmuir, 11 (1995), 33336.

[20] DIMITROV A.S., NAGAYAMA K., Langmuir, 12 (1996), 1303.

[21] DENKOV N.D., VELEV O.D., KRALCHEVAKY P.A., IVANOV I.B., YOSHIMURA H., NAGAYAMA K., Langmuir, 8 (1992), 3183.

[22] HU M., CHUJO S., NISHIKAWA H., YAMAUCHI Y., OKUBO T., J. Nanoparticle Res., 6 (2004), 479.

[23] KO H.-Y., LEE H.-W., MOON, J., Thin Solid Films, 447-448 (2004), 638.

[24] QIN Q., XIA Y., XU B., YANG H., ZHOU C., WHITESIDES M., Adv. Mater. 11 (1999), 1433.